

LA-UR- 98-2200

Approved for public release;
distribution is unlimited.

Title:

AN 800-MeV PROTON RADIOGRAPHY FACILITY
FOR DYNAMIC EXPERIMENTS

CONF-980337--

Author(s):

N.S.P. King, K.R. Alrick, R.A. Gallegos,
N.T. Gray, V.H. Holmes, S.A. Jaramillo,
T.E. McDonald, K.B. Morley, P.D.
Pazuchanics, G.J. Yates (P-23); J.B.
McClelland (P-DO); J.F. Amann, G.E.
Hogan, C.L. Morris, C.M. Riedel, H.-J.
Ziock, J.D. Zumbro (P-25) B.E. Takala
(LANSCE-3); H.E. Tucker, R.K. London
(DX-3); H.L. Stacy, R.P. Lopez (DX-4);
M.L. Crow, T. T. Fife (DX-5); E. Ables,

Submitted to:

THIRD INTERNATIONAL TOPICAL MEETING ON
NEUTRON RADIOGRAPHY NEW DETECTORS,
IMAGING TECHNIQUES AND APPLICATIONS,
3/6/98, LUCERNE, SWITZERLAND; FOR
PUBLICATION IN NUCLEAR INSTRUMENTS AND
METHODS IN PHYSICS RESEARCH, SECTION A

DISTRIBUTION OF THIS DOCUMENT IS UNLIMITED *ph*

MASTER

Los Alamos
NATIONAL LABORATORY

Los Alamos National Laboratory, an affirmative action/equal opportunity employer, is operated by the University of California for the U.S. Department of Energy under contract W-7405-ENG-36. By acceptance of this article, the publisher recognizes that the U.S. Government retains a nonexclusive, royalty-free license to publish or reproduce the published form of this contribution, or to allow others to do so, for U.S. Government purposes. Los Alamos National Laboratory requests that the publisher identify this article as work performed under the auspices of the U.S. Department of Energy. The Los Alamos National Laboratory strongly supports academic freedom and a researcher's right to publish; as an institution, however, the Laboratory does not endorse the viewpoint of a publication or guarantee its technical correctness.

DISCLAIMER

This report was prepared as an account of work sponsored by an agency of the United States Government. Neither the United States Government nor any agency thereof, nor any of their employees, makes any warranty, express or implied, or assumes any legal liability or responsibility for the accuracy, completeness, or usefulness of any information, apparatus, product, or process disclosed, or represents that its use would not infringe privately owned rights. Reference herein to any specific commercial product, process, or service by trade name, trademark, manufacturer, or otherwise does not necessarily constitute or imply its endorsement, recommendation, or favoring by the United States Government or any agency thereof. The views and opinions of authors expressed herein do not necessarily state or reflect those of the United States Government or any agency thereof.

DISCLAIMER

Portions of this document may be illegible in electronic image products. Images are produced from the best available original document.

An 800-MeV Proton Radiography Facility for Dynamic Experiments

N.S.P. King, E. Ables^{*}, Ken Adams, K.R. Alrick, J.F. Amann, Stephen Balzar⁺, P.D. Barnes Jr.^{*}, M.L. Crow, S.B. Cushing, J.C. Eddleman, T.T. Fife, Paul Flores⁺, D. Fujino^{*}, R.A. Gallegos, N.T. Gray, E.P. Hartouni^{*}, G.E. Hogan, V.H. Holmes, S.A. Jaramillo, J.N. Knudsson, R.K. London, R.R. Lopez, T.E. McDonald, J.B. McClelland, F.E. Merrill, K.B. Morley, C.L. Morris, F.J. Naivar, E.L. Parker^{*}, H.S. Park^{*}, P.D. Pazuchanics, C. Pillai, C.M. Riedel, J.S. Sarracino, F.E. Shelley Jr., H.L. Stacy, B.E. Takala, Richard Thompson⁺, H.E. Tucker, G.J. Yates, H.-J. Ziock, and J.D. Zumbro

Los Alamos National Laboratory, Los Alamos, NM 87545, USA

^{*}Livermore National Laboratory, Livermore, CA 94550, USA

⁺Bechtel Nevada, Los Alamos, NM 87545, USA

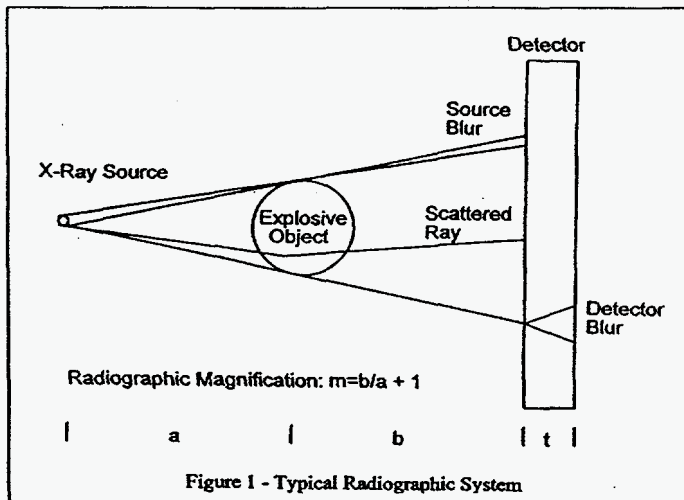
ABSTRACT

The capability has been successfully developed at the Los Alamos Nuclear Science Center (LANSCE) to utilize a spatially and temporally prepared 800-MeV proton beam to produce proton radiographs. A series of proton bursts are transmitted through a dynamically varying object and transported, via a unique magnetic lens system, to an image plane. The magnetic lens system permits correcting for the effects of multiple coulomb scattering which would otherwise completely blur the spatially transmitted information at the image plane. The proton radiographs are recorded on either a time integrating film plate or with a recently developed multi-frame electronic imaging camera system. The latter technique permits obtaining a time dependent series of proton radiographs with time intervals (modulo 358ns) up to many microseconds and variable time intervals between images. One electronically shuttered, intensified, CCD camera is required per image. These cameras can detect single protons interacting with a scintillating fiber optic array in the image plane but also have a dynamic range which permits recording radiographs with better than 5% statistics for observation of detailed density variations in the object. A number of tests have been carried out to characterize the quality of the proton radiography system for absolute mass determination, resolution, and dynamic range. Initial dynamic experiments characterized the temporal and spatial behavior of shock propagation in high explosives with up to six images per experiment. Based on experience with the prototype system, a number of upgrades are being implemented including the anticipated capability for enhanced mass discrimination through differential multiple coulomb scattering radiographs and more images with improved imaging techniques.

INTRODUCTION

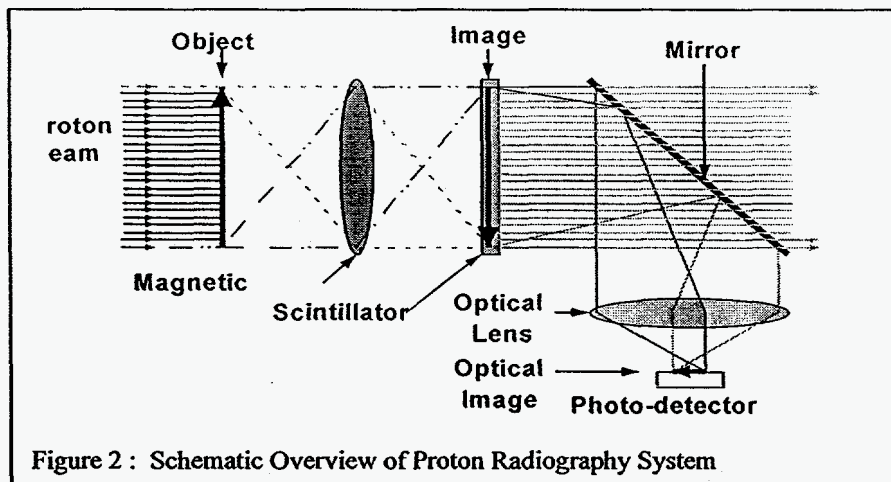
Classical radiography typically involves uncharged incident radiation such as X-rays or neutrons, a portion of which is transmitted through an object of interest to a detector plane as shown in figure 1. Important features of these systems which affect the quality of the resultant projected image onto the detector plane include source size, incident and transmitted flux, detector blur, scattered backgrounds, and detector efficiency. The utility of these radiographs to view various aspects of the object is closely related to the mean free paths for removal of the incident radiation and the interaction of the transmitted flux with the detector. A background from scattering from surrounding material as well as different parts of the object results in reduced contrast. Spatial resolution can be strongly affected by the size of the source as well as the statistics associated with detecting the transmitted radiation. The issue of statistics is compounded by the fact that both neutrons and X-rays are secondary products of primary charged particle production techniques which necessarily results in lower incident fluxes on objects to be radiographed than would be possible using charged particles directly. Problems with low detector efficiencies are also frequently encountered due the necessity of reconvertng incident radiation to charged particle channels. The highly localized energy deposition resulting from the large interaction cross sections for thermal neutrons are an exception.

Obtaining high quality proton radiographs depends upon related but also different issues than for neutral radiation. The fundamental processes for interaction of the incident proton flux are nuclear processes for attenuation, multiple Coulomb scattering(MCS), and energy loss. The latter processes result in additional



complexity in forming a radiograph but can also provide unique possibilities for increased sensitivity to material features in the object. The development and use of magnetic lenses is necessary to compensate for the small angle multiple Coulomb scattering(MCS) which in effect destroys the transmitted "image" through an object. The mean MCS angle is inversely proportional to the incident proton momentum and proportional to the square root of the object thickness. The practical application of proton radiography is therefore a tradeoff between incident momentum and object thickness since the angular acceptance of a lens may become impractical large for low momentum

protons and thick objects. A schematic of a proton radiographic system is presented in figure 2. The image plane detector for our system is either a film plate or a scintillator which is lens coupled to electronic cameras. The 800-MeV proton system at LANSCE permits useful results for $\leq 50\text{g/cm}^2$ objects. It should be mentioned however that much thicker objects can in fact be radiographed but will require increased numbers of protons for good statistics. These numbers can in fact be obtained by increasing the



proton burst width at a sacrifice in temporal resolution. For static radiographs this is not a limitation in any case. An energy selective detector in the image plane can take advantage of differential energy loss for material selection for different regions of an object. A number of such detector options are possible such as those

based on Cherenkov processes but will not be discussed further. The following sections describe current experience with proton radiography at 800-MeV as well as relevant concepts and limitations.

Proton Interaction Processes

The processes which are important to proton radiography are summarized in figure 3. Transmission radiography results from an exponential attenuation of the incident proton flux by nuclear processes which contribute to the mean free path for removal of a proton from the detection system. This can include the fraction of nuclear elastic scattering not collected by the magnetic lens system. Coulomb multiple scattering at large angles can also effectively remove a fraction of the transmitted protons from the image plane. This feature is one which can provide a unique capability for proton radiography. The detector in the initial image plane can be constructed to permit further transport of the "image" protons through a second magnetic lens system which has a smaller angular acceptance which then preferentially removes protons having the largest MCS angles in a second image plane. These image regions will correspond to

those object areas containing more dense or possibly higher Z materials. It should be mentioned that the detector systems for protons can be made highly efficient in that charged particle detection is dependent upon Coulomb interactions rather than through the formation of secondary charged particles as in the case

TRANSMISSION	MULTIPLE SCATTERING
$\frac{N_1}{N_0} = e^{-\sum \frac{l_i}{\lambda_i}}$	$\frac{N_2}{N_1} = \frac{1}{2\pi\theta_0^2} \int_0^{\theta_0} e^{-\frac{e^2}{2\theta_0^2}} d\Omega \equiv \left[1 - e^{-\frac{e^2}{2\theta_0^2}} \right]$
so, $\sum \frac{l_i}{\lambda_i} = -\ln\left(\frac{N_1}{N_0}\right)$	where, $\theta_0 \approx \frac{14.1}{p\beta} \sqrt{\sum \frac{l_i}{L_{ri}}}$
	so, $\sum \frac{l_i}{L_{ri}} = -\frac{(p\beta\theta_m)^2}{2(14.1)^2 \ln\left(1 - \frac{N_2}{N_1}\right)}$

Figure 3. Proton Radiography Processes

of X-rays or neutrons. This results in the potential for making images with very high statistics for a relatively small number of transmitted particles since each proton can in principle be detected.

Magnetic Lens and Proton Beam Properties

The magnetic lens system utilized in 800-MeV proton radiography at LANSCE is shown in figure 4. A diffuse beam is generated over the object plane by

introducing adjustable thickness stainless steel ($\leq 1.5\text{mm}$) at a location upstream from a quadrupole magnet pair. This results in a divergent beam in the horizontal plane and convergent beam in the vertical plane with a specific correlation between positions and angle at the object location.

The protons transmitted through the object are transported by the "lens" system consisting of four matched quadrupoles to the image plane with a magnification of minus one. This condition is chosen to minimize chromatic aberrations and results in uniform acceptance over the field of view. The entire

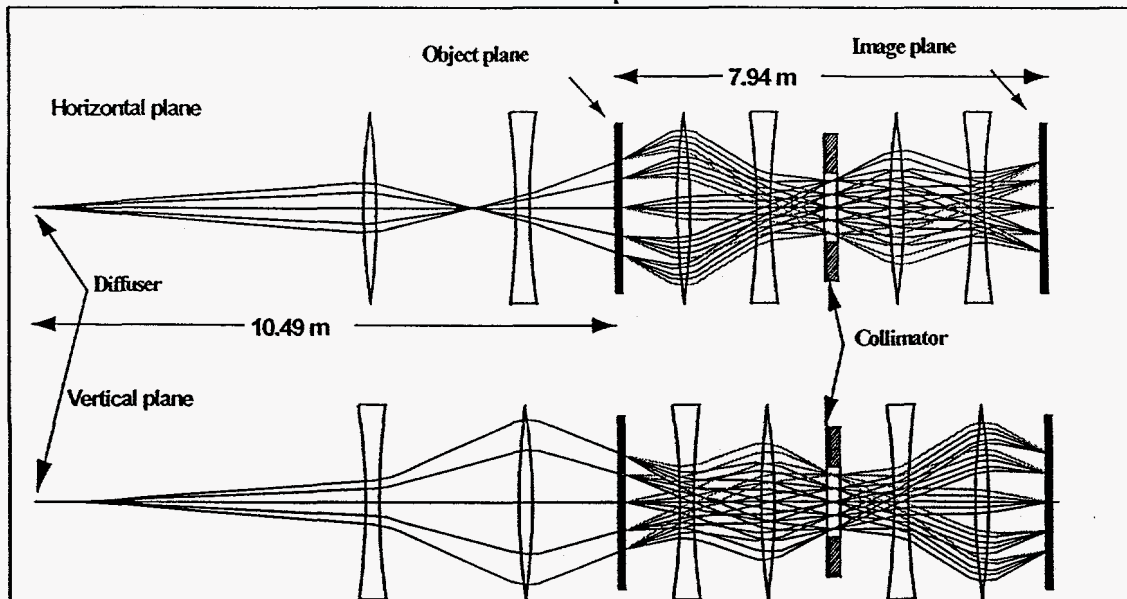


Figure 4. X- and Y- plane ray traces for the magnetic lens system used in the experiment. The incident proton beam was expanded with a diffuser and an upstream lens set, which also established a correlation between particle location and angle at the object plane. The correlation reduced aberrations in the subsequent inverting identity lens. The identity lens consisted of four quadrupole magnets. Multiple Coulomb scattering of the proton beam by the object is schematically indicated. Scattered rays are at angles of ± 10 , ± 5 , and 0 mrad with respect to a "nominal" ray. The radial angle sorting at the midplane of the lens (collimator location) is clearly evident. (The transverse scale is greatly expanded relative to the longitudinal scale in which a magnetic aperture is 20cm)

magnetic lens system can be approximated by simple ray tracing of "optical" rays much like a pinhole or simple lens located at the center of the lens. More details can be found in reference 1. The depth of field for this system can be estimated from the angular acceptance of such a simple lens geometry and results in about a $\pm 25\text{mrad}$ correlation angle in the image plane for the horizontal (vertical) plane at the edge of the field of view. This results in a projected resolution of about 2lp/mm for the extreme rays at the edge of the

field of view for an image plane depth of 2 cm. This scales to about 4lp/mm for a central field of view of 6.4cm. Added to this resolution is the angular spread about each central ray trajectory due to the maximum MCS angle. This is limited by the collimator at the center of the quadrupole pairs and is typically $\pm 10\text{mr}$ as well. The final resolution is then a convolution of these effects.

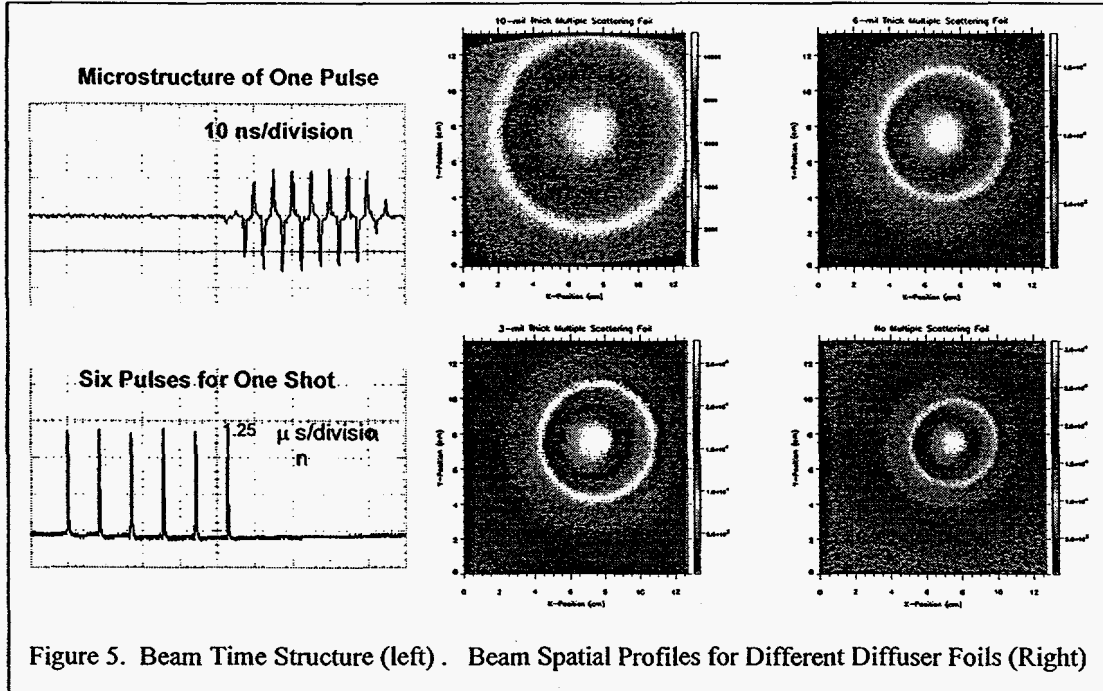


Figure 5. Beam Time Structure (left) . Beam Spatial Profiles for Different Diffuser Foils (Right)

Typical beam profiles for a burst of 7 proton pulses (200ps/pulse) are shown in figure 5. The beam area is contained within a $12 \times 12 \text{ cm}^2$ field of view. The number of protons per pulse is typically 5×10^8 . The capability of generating a series of proton bursts, each containing a programmable number of

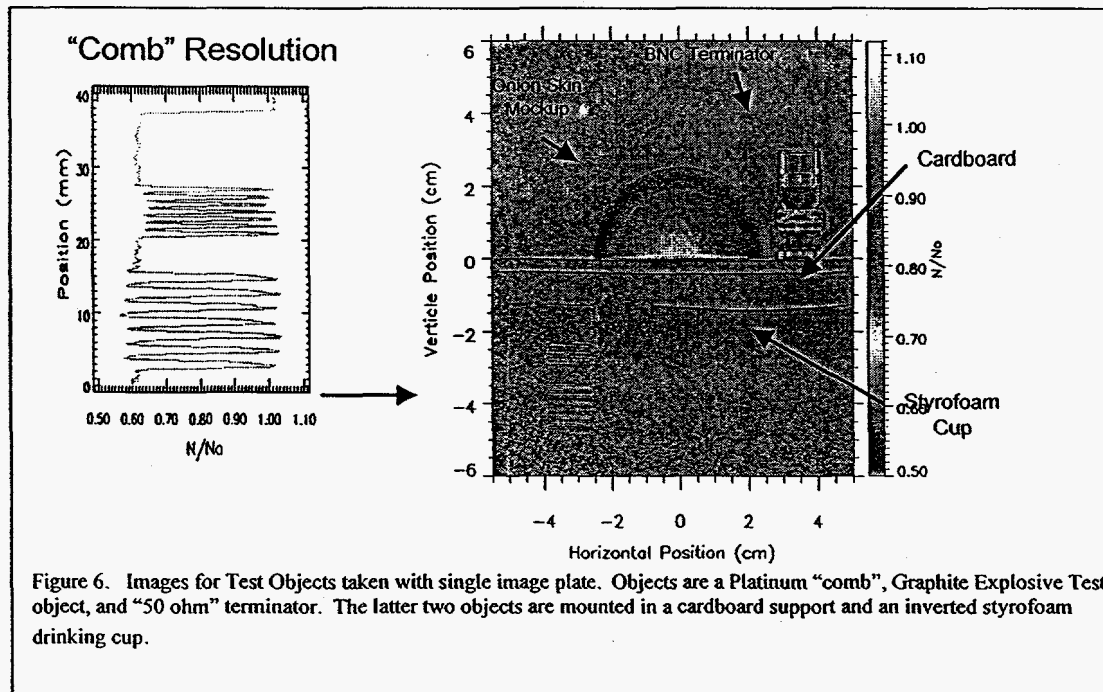


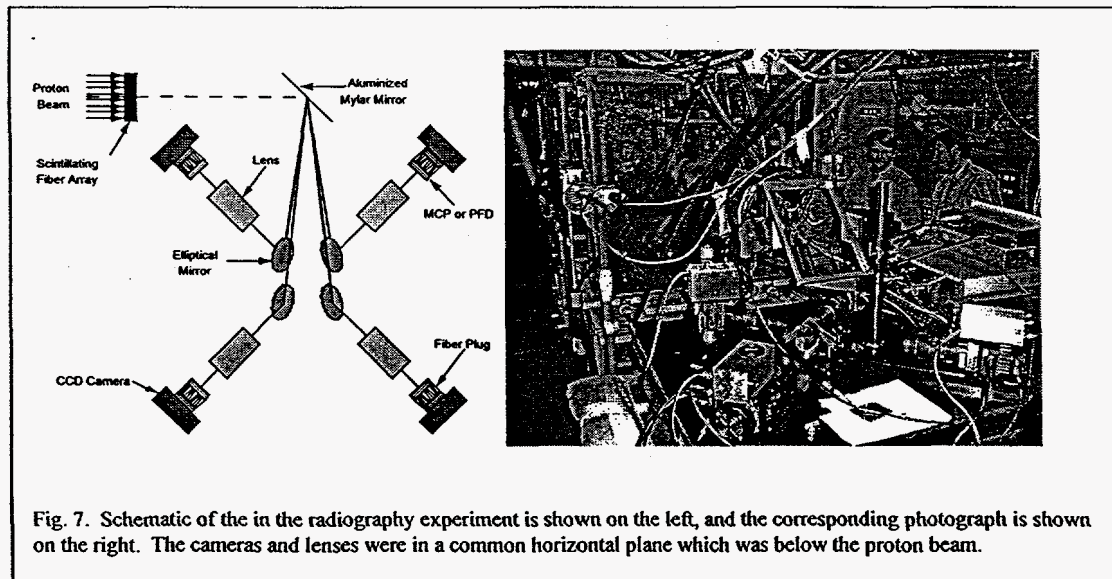
Figure 6. Images for Test Objects taken with single image plate. Objects are a Platinum "comb", Graphite Explosive Test object, and "50 ohm" terminator. The latter two objects are mounted in a cardboard support and an inverted styrofoam drinking cup.

micropulses permits varying both the "exposure" time per image as well as the option of multiple images at different times. The imaging detector system utilizing electronic cameras can be shuttered to isolate different images corresponding to different proton bursts. The film plates give a "time integrated" image.

A typical burst pattern of 50ns width can be repeated as frequently as 358ns. Longer separations with non-uniform spacing are possible in multiples of 358ns. The 358ns minimum time separation between bursts and the multiplying factor for multiple bursts is a current feature of our accelerator pulse programmer and not a fundamental limitation of the LANSCE accelerator system.

Image Plane Detectors

Image plane detector system requirements are dictated by a desire to exceed the resolution obtainable from the other radiographic system components such as the magnetic lens. The object plane field of view has a diameter of 127mm and is equal to that in the image plane for a magnetic lens magnification of -1.0 . The detailed, non-image plane resolution performance is complicated in that it depends to some extent on energy loss effects which are object specific and requirements for entrance and exit windows in a containment system for high explosive (HE) experiments. Data obtained with a large format, phosphor image plate system with a resolution close to 10lp/mm permits evaluating resolution effects for a number of simple objects. These static images are not limited by statistics associated with the number of transmitted protons. The image plates have an efficiency of about 50% per proton. The response of the image plate system to varying radiation intensity was evaluated with a radioactive source. No corrections were found necessary to permit obtaining quantitative radiographic density variations better than 5%. An example of a single image plate radiograph is shown in figure 6. The resolution object is a 2mm thick platinum "comb" in which the finest spacings are 0.5mm. The system resolution is clearly much better than this. The "Onion Skin" explosive mockup is a graphite hemisphere with a 0.25mm aluminum shell imbedded in it to simulate a 30% higher density high explosive "burn front". Initial dynamic experiments involved explosive assemblies similar to this which were placed in a 122cm diameter steel, containment vessel with entrance and exit pipes for the proton beam. The entrance pipe had an 1.27cm thick aluminum entrance window and the exit pipe extended through the lens system to a 1.27cm exit window within 1cm of the image plane. Image plates were mounted to the exit window for static or single image radiographs. For electronic imaging a 2.5cm thick scintillating fiber array was placed at the



exit window. This array was made from 300micron core, circular fibers with a time response of about 3.5ns. As shown in figure 7, the light from from the array was reflected into multiple, gated, intensified, cooled CCD cameras. The number of protons per experiment was low enough that radiation shielding of the camera system was not needed. All cooled, CCD cameras were fiber optically coupled to their respective gated intensifiers. Different gated intensifier, CCD camera combinations were utilized with Nikon 105mm f1.8 or 135mm f2.0 lenses. The intensifiers served the purpose of providing necessary optical shuttering and wavelength shifting from the 415nm scintillator light to a P43 phosphor light which has a high quantum efficiency for detection by the CCD arrays. Proven 200 Volt gating techniques with microchannel plate image intensifiers (MCP) were used as well as new 10 Kilovolt gates on planar diodes.

Typical optical shutter times were 350ns. Transmitted fluxes of 10^5 protons/mm² in the image plane for a 50ns burst resulted in 60% full pixel well signals for the planar diode gated, 1024x1024, CCD pixel arrays. Very low gains were required in the MCP-II based systems to avoid saturation of their 512x512 pixel CCD arrays. As a consequence, the MCP-II based systems had poorer signal to noise characteristics compared to the planar diode based cameras. This is the result of a loss in photoelectrons due to the MCP prior to the P43 phosphor screens. Based on a statistical analysis of a series of images, a detection quantum efficiency (DQE) of 0.6 and 0.4 were obtained for the planar diode/1024pixel and MCP-II/512pixel camera systems.

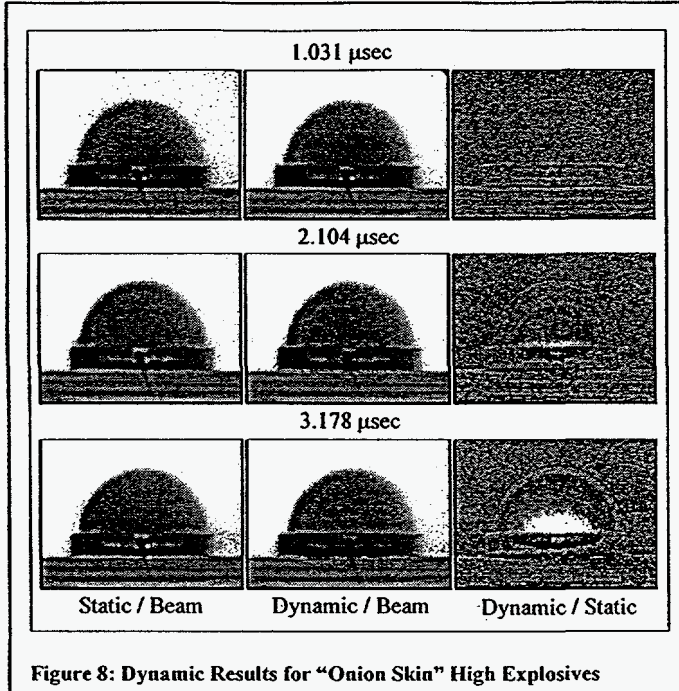


Figure 8: Dynamic Results for "Onion Skin" High Explosives

the dynamic sequence and the corresponding camera static image with the object present. A series of five static images with the object present were recorded just prior to

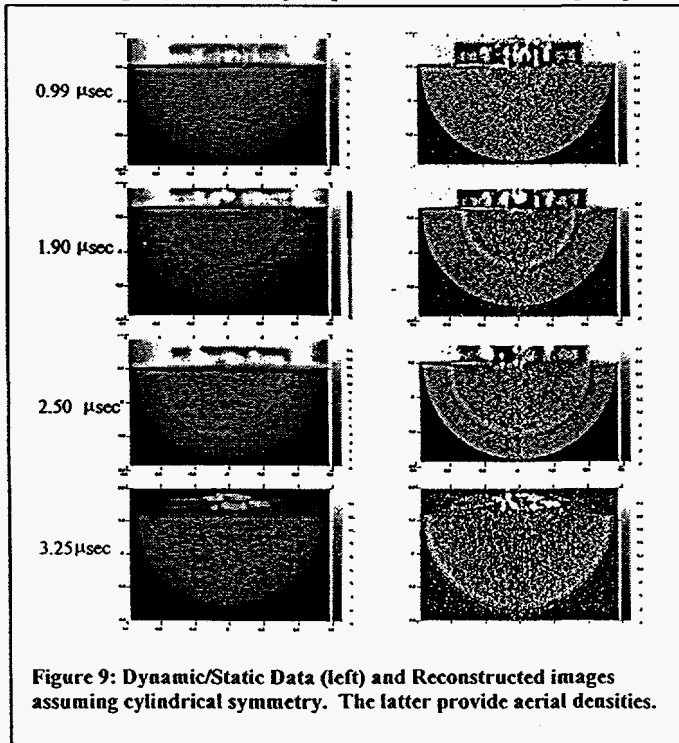


Figure 9: Dynamic/Static Data (left) and Reconstructed images assuming cylindrical symmetry. The latter provide aerial densities.

This can be related to the number of detected photoelectrons per proton being 1.5 and 0.66 respectively. A dynamic range of $\geq 10^4:1$ has been measured for the camera systems. More details on the electronic system are given in reference 2.

DYNAMIC RESULTS

An example of three images from three gated cameras is shown in figure 8. The first column corresponds to the ratio between a static image with and without the object present. The second column is a ratio between a series of dynamic images taken at the times noted and the same image used in the first column without the object present. Shutter widths were 350ns as mentioned previously with a proton burst width of 50ns. The last column is a ratio between the dynamic sequence and the corresponding camera static image with the object present. A series of five static images with the object present were recorded just prior to igniting the high explosive to obtain the dynamic results. The static image used was an average of the five static images taken to improve the signal to noise. One can clearly see the evolution of the high explosive burn front from the top to bottom images.

A second series of images taken with film plates in four successive experiments is shown in figure 9. The first column is a ratio of static to dynamic data and is similar to the third column in the previous figure. A reconstruction algorithm assuming cylindrical symmetry has been used to obtain density slices from the experimental aerial densities. These slices clearly show the desired temporal behavior of the "burn front" density variations needed to provide quantitative information for improving high explosive models.

CONCLUSIONS

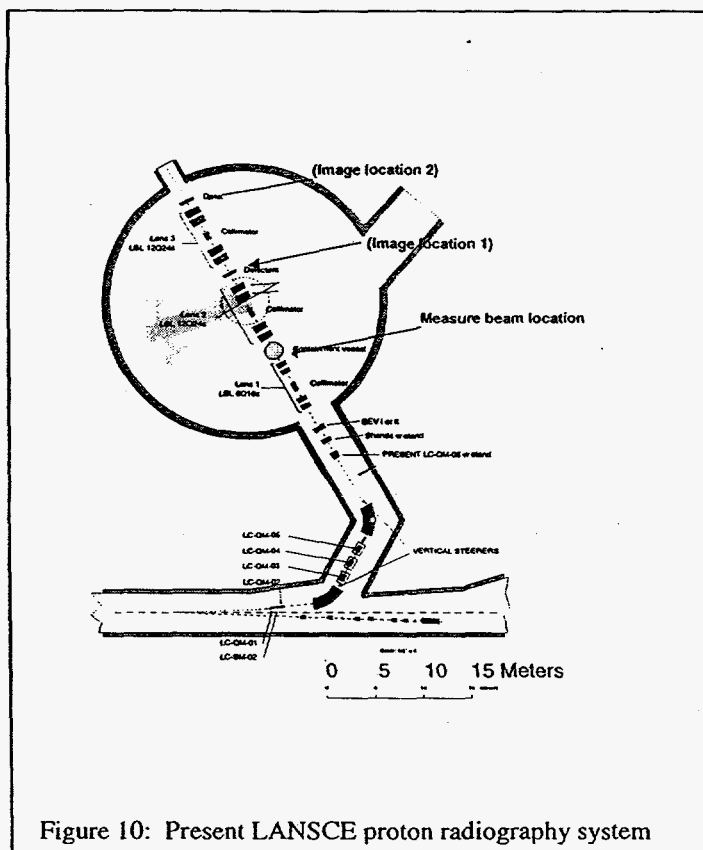


Figure 10: Present LANSCE proton radiography system

provide a magnification of 4:1 for enhanced resolution requirements.

A series of static and dynamic experiments have been performed to demonstrate the possibility of utilizing 800-MeV protons to obtain radiographs of high quality. Unique features of high statistics, high detection efficiency, and multiple pulses with a high resolution magnetic lens provide a powerful, quantitative tool for radiographic experiments. Resolution of ≤ 200 microns has been achieved with time response ≤ 50 ns. The current system for 800-MeV radiography is shown in figure 10. This is an upgrade to the previous system used in initial experiments in that it contains a multiple lens system to vary the accepted multiple scattering angle for enhanced material identification in two image planes. Different collimator sizes will permit obtaining two radiographs per proton pulse in two image planes. The incident beam profile can also be captured on a pulse by pulse basis for normalization purposes. Seven individual cameras per image plane based on gated planar diodes provide the electronic images. It is anticipated that the magnetic lens can be operated to

REFERENCES

- ¹ C.T. Mottershead and J. D. Zumbro, "Magnetic Optics For Proton Radiography", Proceedings of the Particle Accelerator Conference, Vancouver, Canada, May 1997
- ² G.J.Yates et al, "An intensified/shuttered cooled CCD camera for dynamic proton radiography", Proceedings of Electronic Imaging '98 Conference, 24-30 January 1998, San Jose, CA.